Spike-evoked suppression and burst patterning in dorsal root ganglion neurons of the rat

Ron Amir and Marshall Devor *

Department of Cell and Animal Biology, Life Sciences Institute, Hebrew University of Jerusalem, Jerusalem 91904, Israel

1. A low level of spontaneous impulse discharge is generated within dorsal root ganglia (DRGs) in intact animals, and this activity is enhanced following nerve injury. Many physiological stimuli present *in vivo* are capable of augmenting this ectopic discharge. Whatever their cause, episodes of sharply accelerated DRG firing tend to be followed by 'after-suppression' during which discharge falls below baseline rate. In this study we examined the process of postexcitation suppression of firing rate, and how it shapes spike patterning in primary sensory neurons.

2. We recorded intracellularly from sensory neurons in excised rat DRGs *in vitro*. Trains of spikes triggered by intracellular current pulses evoked a prolonged hyperpolarizing shift. This shift appeared to be due to activation of a Ca^{2+}-dependent K^+ conductance ($g_{K(Ca)}$). Spikes evoked by just-suprathreshold pulses triggered a hyperpolarizing shift and spike cessation. As the shift decayed, spiking was restored. The net result was bursty (on–off) discharge, a previously unexplained peculiarity of ectopic discharge in some DRG neurons *in vivo*.

3. Conditioning nerve tetani delivered to axons of neurons which share the DRG with the impaled neuron evoked transient depolarization ('cross-depolarization'). However, when stimulus strength was increased so as to include the axon of the impaled neuron, the net result was a hyperpolarizing shift. Nerve stimulation that straddled the threshold of the axon of the impaled neuron drove it intermittently, but it always drove axons of at least some neighbouring neurons. The result was dynamic modulation of the membrane potential of the impaled neuron as cross-depolarization and spike-evoked hyperpolarizing shifts played off against one another. Membrane potential shifted in the hyperpolarizing direction whenever the axon was activated, and shifted in the depolarizing direction whenever it was silent. Dynamic modulation of this sort probably also occurs *in vivo* when stimuli are drawn over the surface of the skin.

Recent evidence indicates that impulse discharge in primary afferent neurons may be generated ectopically within the dorsal root ganglia (DRGs), in addition to the normal site of electrogenesis in the peripheral sensory endings (Wall & Devor 1983; Burchiel, 1984*a*; Study & Kral, 1996). Such ectopic afferent activity occurs in the intact system, but is enhanced following nerve injury (Wall & Devor, 1983; Burchiel, 1984*b*; Kajander, Wakisaka & Bennett, 1992; Study & Kral, 1996). The functional role of this anomalous DRG firing, if any, is unknown. It has been suggested, however, that it might contribute to a background sense of body image, and that its enhancement in neuropathy might contribute to hyperalgesia, dysaesthesia and on-going pain (Sheen & Chung, 1993; Devor, 1994, 1996; Yoon, Na & Chung, 1996). These considerations motivate an investigation of the factors that modulate spike generation in the DRG.

Various physiological stimuli, present *in vivo*, are capable of accelerating ectopic DRG discharge. For example, afferent activity from the skin and electrical stimulation of afferent axons can enhance spike discharge in neighbouring DRG afferents that were not stimulated directly (DRG 'cross-excitation'; Devor & Wall, 1990; Amir & Devor, 1996). Likewise, sympathetic efferent activity can excite DRG firing (Devor, Janig & Michaelis, 1994; Xie, Zhang, Petersen & La Motte, 1995), as can mechanical displacement, ischaemia and various depolarizing drugs (Howe, Loeser &

* To whom correspondence should be addressed.

Calvin, 1977; Wall & Devor, 1983; Burchiel, 1984*a*, *b*; Devor & Wall, 1990).

Whatever their cause, episodes of sharply accelerated DRG firing are usually followed by a period of after-suppression, lasting for up to tens of seconds, during which discharge rate falls below baseline and may even cease entirely (e.g. Fig. 2 in Devor & Wall, 1990; Fig. 3 in Devor *et al.* 1994). Recovery to the baseline firing rate occurs only at the end of this period of after-suppression. The aim of the present study was to clarify the mechanism(s) responsible for this postexcitation firing rate suppression. In particular, we asked whether after-suppression is a direct effect of the process (e.g. neurotransmitter) responsible for the excitation, or whether it is secondary to the acceleration of spike firing. We have focused in particular on the after-suppression that follows mutual cross-excitation within DRGs. The main conclusion was that after-suppression is not a direct effect of the DRG cross-excitation process, but rather, is an outcome of accelerated impulse discharge. It is a reasonable inference that this is so also for other excitatory conditions noted above.

METHODS

Animals and preparation

The experiments were carried out using fifty-three young rats (33 males, 20 females; 2–6 weeks old; 15–145 g) of the Wistar-derived Sabra strain (Lutzky, Aizer & Mor, 1984). The animals were deeply anaesthetized with pentobarbitone sodium (Nembutal, 60 mg kg^{-1}, I.P.) and killed by carotid exsanguination. DRGs L4 or L5 were excised with their dorsal roots (DRs), the spinal nerve and a variable length of attached sciatic nerve. After about 1 h of recovery in a modified Krebs solution (containing (mM): NaCl, 124; $NaHCO_3$, 26; KCl, 3; NaH_2PO_4, 1·3; $MgCl_2$, 2; dextrose, 10; and saturated with 95% O_2 and 5% CO_2; pH 7·4; 290–300 mosmol l^{-1}; 20 °C), the ganglia were mounted in a recording chamber and superfused with the Krebs solution (1–2 ml min^{-1}, 20 or 37 °C) to which 2 mM $CaCl_2$ was added. In experiments in which Ca^{2+} channel blockers were used, the $CaCl_2$ was replaced by $CoCl_2$ or $NiCl_2$. In some experiments the Ca^{2+}-dependent K^+ conductance ($g_{K(Ca)}$) blocker apamin (5 nM; Alomone Laboratories, Jerusalem, Israel) was added to the standard or Ca^{2+}-free Krebs solution.

Sharp glass microelectrodes were used for intracellular recording and stimulation (20–40 MΩ filled with 3 M KCl or 2 M potassium acetate). The electrodes were passed through the undissected DRG capsule, which is thin in young rats. All cells reported here had a stable resting membrane potential which was more negative than −40 mV and, on intracellular somatic or extracellular axonal stimulation, an overshooting spike. Data were recorded digitally on magnetic tape for off-line analysis.

Cell samples

The preparation did not permit the determination of receptive fields (RFs). We categorized neurons by axonal conduction velocity (v_c) and the shape of the intracellularly recorded spike. v_c was calculated by dividing the propagation distance by the spike latency following single suprathreshold stimulus pulses to the sciatic nerve or the DR. For present purposes, if the v_c was > 1 m s^{-1}, the neuron was categorized as having a myelinated axon (A-neuron), regardless of temperature or the age of the animal. The minority of neurons for which v_c was not determined were categorized as A- or C-neurons based on a combination of spike shape and width, as described elsewhere (Amir & Devor, 1996).

Electrophysiological recording

Three alternative protocols were used to deliver conditioning tetani to the axons of neighbouring DRG neurons while avoiding the axon of the impaled neuron. The results obtained were comparable. (1) By adjusting current strength and polarity the DR was stimulated (DRS) just-subthreshold for the impaled neuron, but suprathreshold for many neighbours as judged from the size of the compound action potential (CAP) monitored through a suction electrode on the sciatic nerve. (2) Pulses subthreshold for the impaled neurons were delivered to the sciatic nerve (SN) while the CAP was monitored from the DR. (3) The DR was split longitudinally and stimuli were delivered to each branch separately. Conditioning tetani were delivered to the branch which, when stimulated, did not evoke a soma spike.

Nerve/DR stimuli were monophasic 0·1–0·2 ms square pulses, ≤ 7 mA, delivered singly or in 10 s tetani at 10–500 Hz (usually 50 and/or 100 Hz). Two to sixteen repeated trials were run for each set of stimulus parameters for a given cell. The stimulus parameters used were not sufficient to activate unmyelinated axons as judged both from the CAP and the failure to record evoked spikes from neurons with unmyelinated axons. To stimulate the impaled neuron, in isolation from its neighbours, intracellular depolarizing pulses were applied through the amplifier bridge circuit (1–40 ms, 0·1–8·0 nA, 1–200 Hz).

To test whether conditioning tetani produce a change in whole-cell membrane conductance, the amplifier bridge was carefully balanced and constant current hyperpolarizing pulses (0·5–2 nA, 20–100 ms, usually ≥ 80 ms) were delivered intracellularly at 2 Hz. Input resistance (R_{in}) was calculated from the voltage peak using Ohm's law.

To measure cell excitability, we monitored changes in the proportion of test pulses which evoked a spike during 10 s periods of fixed-intensity 1 or 2 Hz intracellular stimulation ('firing probability' = n responses per 10 or 20 test stimuli). To check for excitation, stimulus intensity was initially set at just below (~15%) threshold so that the pre-conditioning firing probability was 0/10 or 0/20. A significant increase indicated excitation (criterion for $P < 0·05$ was ≥3/10 or ≥5/20; one-tailed Fisher's test). Suppression was checked using just-suprathreshold test pulses (the minimal current required to achieve a firing probability of 20/20), and determining whether the firing probability decreased during or after the conditioning tetanus (criterion for $P < 0·05$ was ≤15/20). In some experiments firing probability was initially set between 0/20 and 20/20. In this way excitation and suppression could be monitored in the same trial by obtaining an increase or a decrease in firing probability (two-tailed Fisher's test). Stimulus pulse duration was always much longer than the chronaxie for these cells (1·8 ± 0·4 ms; $n = 25$), and therefore changes in firing probability could not have reflected subtle, uncontrolled changes in effective pulse width.

All means are given ± the standard deviation (S.D.). Unless otherwise noted, statistical evaluations are based on Student's t tests, Mann–Whitney U tests, and the significance of linear correlation coefficients (criterion $P < 0·05$).

Table 1. Amplitude and duration of the brief and the prolonged phases of after-hyperpolarization in A_0 and A_{inf} neuron soma spikes at 20 and 37 °C

Neuron type	Temperature (°C)	Brief AHP		Prolonged AHP		Ratio of cells with both brief and prolonged AHP
		Amplitude (mV)	Duration (ms)	Amplitude (mV)	Duration (ms)	
A_0	20 and 37	12·6 ± 4 (86)	6·4 ± 3·6 (86)	2·1 ± 1·8 (15)	333 ± 308 (15)	16/88 (18%)
A_{inf}	20 and 37	11·3 ± 4·3 (40)	8·5 ± 3·5 (40)	2·7 ± 1·5 (33)	382 ± 282 (33)	41/48 (85%)
A_0 *vs.* A_{inf}		$P > 0·05$	$P < 0·01$	$P > 0·05$	$P > 0·2$	$P < 0·0001$ *
A_0	20	10·2 ± 3·0 (20)	7·7 ± 3·2 (20)	—	—	1/21 (5%)
A_{inf}	20	8·0 ± 3·0 (5)	7·0 ± 2·1 (5)	2·1 ± 0·9 (4)	253 ± 171 (4)	5/6 (83%)
A_0	37	13·3 ± 4·1 (66)	6·0 ± 3·6 (66)	2·1 ± 1·8 (15)	333 ± 308 (15)	15/67 (22%)
A_{inf}	37	11·8 ± 4·3 (35)	8·7 ± 3·7 (35)	2·8 ± 1·5 (29)	399 ± 292 (29)	36/42 (86%)
Both	20	9·8 ± 3·1 (25)	7·5 ± 3 (25)	2·1 ± 0·9 (4)	253 ± 171 (4)	6/27 (22%)
Both	37	12·8 ± 4·2 (101)	6·9 ± 3·9 (101)	2·6 ± 1·6 (44)	377 ± 295 (44)	51/109 (47%)
20 *vs.* 37 °C		$P < 0·001$	$P > 0·2$	$P > 0·2$	$P > 0·2$	$P < 0·05$ *
All conditions		12·2 ± 4·2 (126)†	7·0 ± 3·7 (126)	2·5 ± 1·6 (48)	367 ± 288 (48)	57/136 (42%)

Values are means ± S.D. * indicates two-tailed Fisher's test. All other tests were Mann–Whitney *U* tests. † includes cells with and without a prolonged AHP. Numbers in parentheses in columns 3–6 are *n*, the number of cells tested.

RESULTS

We report here on observations from A-neurons; corresponding data from C-neurons will be presented elsewhere. Just over one-third of the neurons examined (35%, Table 1) had an inflection on the falling phase of the spike (A_{inf} neurons), as determined using an analog signal differentiator. The majority did not show this inflection (A_0 neurons). The A_0 group had a faster v_c than the A_{inf} group (7·0 ± 2·3 *vs.* 5·3 ± 2·7 m s^{-1}, $P < 0·01$). The A_0 group is presumed to represent predominantly Aβ afferents, most of which are low threshold mechanoreceptors; the A_{inf} group, containing many Aδ afferents, probably includes most of the myelinated nociceptors (Gorke & Pierau, 1980; Koerber & Mendell, 1992; Villiere & McLachlan, 1996).

After-hyperpolarization following a single spike

The soma spike evoked by single intracellular stimulus pulses, or by axonal stimulation, was nearly always followed by an after-hyperpolarization (AHP; 135 of 136 cells tested; 87 A_0 neurons, 48 A_{inf} neurons). In the majority of neurons tested, the AHP was large and brief (58% of cells sampled; 10·4 ± 4·1 mV, < 20 ms; decay time constant (τ_{decay}) = 3·2 ± 1·4 ms). In just under half of the neurons (42%), the AHP had two phases (Fig. 1*A* and *B*). The first phase was large and brief, the second phase was prolonged and of smaller amplitude (2·5 ± 1·6 mV; range, 30–2000 ms; τ_{decay} = 156·9 ± 114·4 ms; Table 1). The one A_0 cell with no AHP had a brief (15 ms) after-depolarization. We have also encountered cells with a brief (a few milliseconds) depolarizing after-potential following their AHP and occasional cells with delayed AHPs lasting for up to 10 s (Fig. 1*C*).

Prolonged AHPs were more common in A_{inf} than in A_0 cells, and at 37 °C than at 20 °C (Table 1). However, there was no significant correlation between the duration of the prolonged AHP and spike duration ($r = -0·005$, $P > 0·2$), v_c ($r = 0·18$, $P > 0·2$), or resting membrane potential ($r = -0·1$, $P > 0·2$).

Hyperpolarizing shift evoked by repetitive spiking

The entire sample of neurons was tested with 1 or 2 Hz intracellular stimulus trains. In the large majority evoked spikes were followed by an AHP ≪ 500 ms in duration and there was no indication of an interaction from one spike to the next. However, about 10% had particularly prolonged AHPs which summated resulting in a steady-state hyperpolarizing shift (Fig. 2*A*).

Increasing stimulation frequency to 5–200 Hz (2–15 s trains) yielded a hyperpolarizing shift in nearly all neurons tested (41 of 42). In many cells the shift occurred even when the AHP was shorter than the interval between stimulus pulses, suggesting that temporal summation of AHPs may not fully account for the hyperpolarizing shift. The shift began with the first stimulus pulse in cells with prolonged AHP (Fig. 2*C*), or more gradually during the first several stimulus

pulses (Fig. 2*B*). A plateau of 0·5–10 mV was reached after a few seconds of stimulation. The plateau was usually stable, but in several cells it sagged even though the cell continued to fire. The peak amplitude of the hyperpolarizing shift, its time to onset, rate of rise, and time to recovery all depended on stimulation frequency and cell type. Most notably, the shift was larger and more prolonged in A_{inf} than in A_0 neurons (Table 2).

At the end of the stimulus train membrane potential usually recovered directly to baseline (over 0·5–50 s; $\tau_{decay} = 2{\cdot}6 \pm 4{\cdot}5$ s; e.g. Figs 2 and 3*A*, left). However, in four of the forty-two neurons tested, all A_0, there was a rebound depolarizing shift following the tetanus ($\leqslant 3$ mV, $\leqslant 7$ s), and in another four (3 A_0, 1 A_{inf}) hyperpolarization was replaced by depolarization even before the end of the tetanus (Fig. 3*A*, right, and *B*).

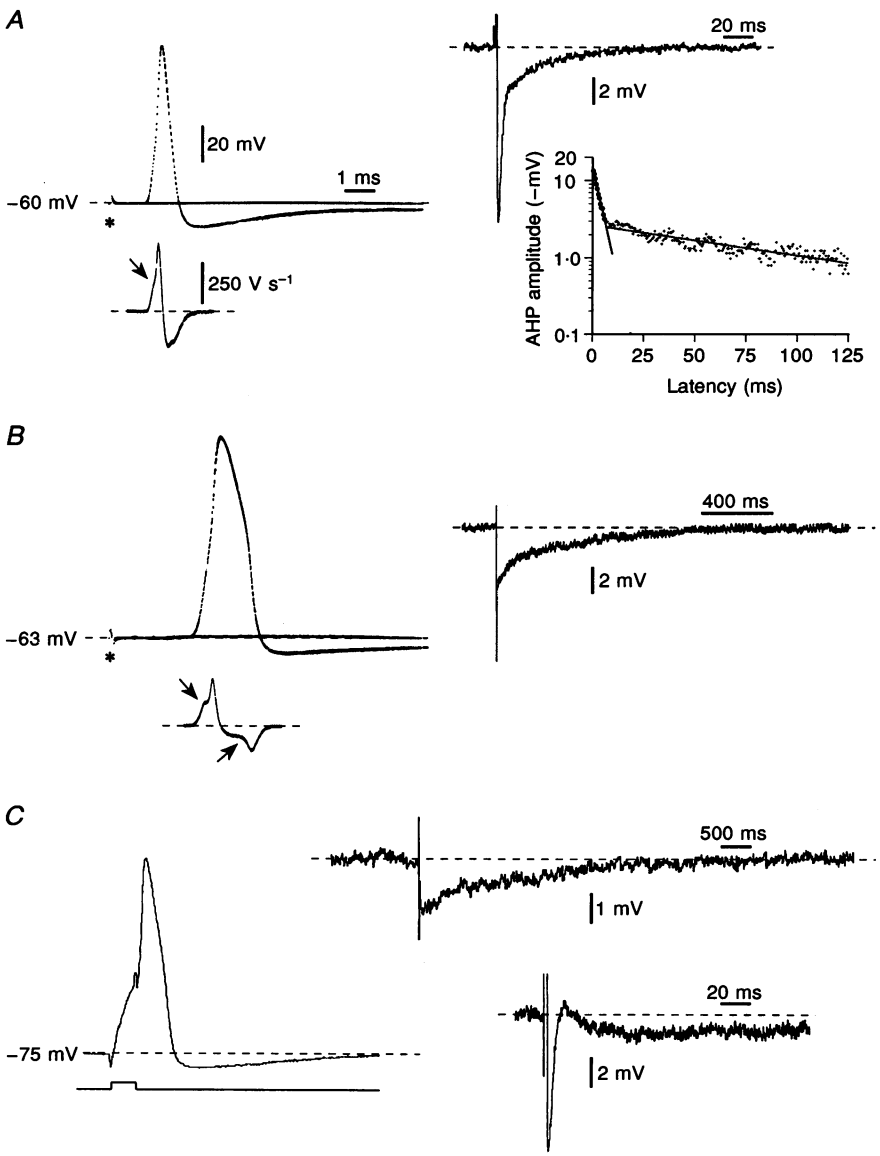

Figure 1. Spike waveform and after-hyperpolarization in A_0 and A_{inf} neurons

In *A* and *B* the axon was stimulated (*) just below and just above threshold (single sweeps). Upper traces show the spike waveforms of A_0 (*A*) and A_{inf} neurons (*B*). Lower traces show the differentiated voltage signal illustrating spike inflections (arrows). The higher gain, slower time base records on the right illustrate the two phases of the AHP, including a log plot for the cell in *A* with linear regression plots for the two phases (1·5 and 0·2 mV ms^{-1}). *C*, the spike waveform of an A_{inf} neuron, stimulated intracellularly, in which the spike is followed by a depolarizing after-potential and afterwards by a prolonged AHP which lasted for nearly 5 s.

Effect of g_{Ca} and $g_{K(Ca)}$ blockers

AHP following a single spike

Bath application of the Ca^{2+} channel blockers Co^{2+} (2·5 or 5·0 mM) or Ni^{2+} (2 mM) abolished or significantly attenuated the post-spike AHP (6 of 9 cells; 1 of 2 A_0, 5 of 7 A_{inf}); the $g_{K(Ca)}$ blocker apamin (5·0 nM) did likewise (5 of 5 cells; A_0, 4 A_{inf}; Fowler, Greene & Weinreich, 1985; Luscher, Streit, Lipp & Luscher, 1994). In six of these fourteen cells elimination of the AHP revealed an after-depolarization (Fig. 4).

Hyperpolarizing shift

Ni^{2+} and Co^{2+} also reduced or abolished the hyperpolarizing shift evoked by repetitive spiking (8 of 8 cells; $-3·9 \pm 2·4$ mV before *vs.* $0·2 \pm 1·4$ mV after application of the blockers, $P < 0·01$, Fig. 4*A*). This includes one A_0 neuron that did not have a prolonged AHP. In two cells treated with Co^{2+} tetanic stimulation evoked depolarization similar to that shown in Fig. 3, but in the absence of a prior hyperpolarizing shift. Such depolarizing shifts following repetitive spiking have been reported previously in rat DRG neurons by Mayer (1985) who attributed them to a Ca^{2+}-activated Cl^- current. The fact that in our study depolarizing shifts were seen in the presence of g_{Ca} blockers indicates that a different, non-Ca^{2+}-dependent process is involved. A likely possibility is K^+ accumulation in the narrow space between the soma and the satellite cell sheath (Luscher *et al.* 1994; Shinder & Devor, 1994). Apamin also diminished or completely abolished the hyperpolarizing shift (5/5 cells; $-5·3 \pm 2·0$ mV before *vs.* $-0·6 \pm 0·9$ mV after application of apamin, $0·1 > P > 0·05$; Fig. 4*B*). These changes developed gradually over a period of about 5–10 min.

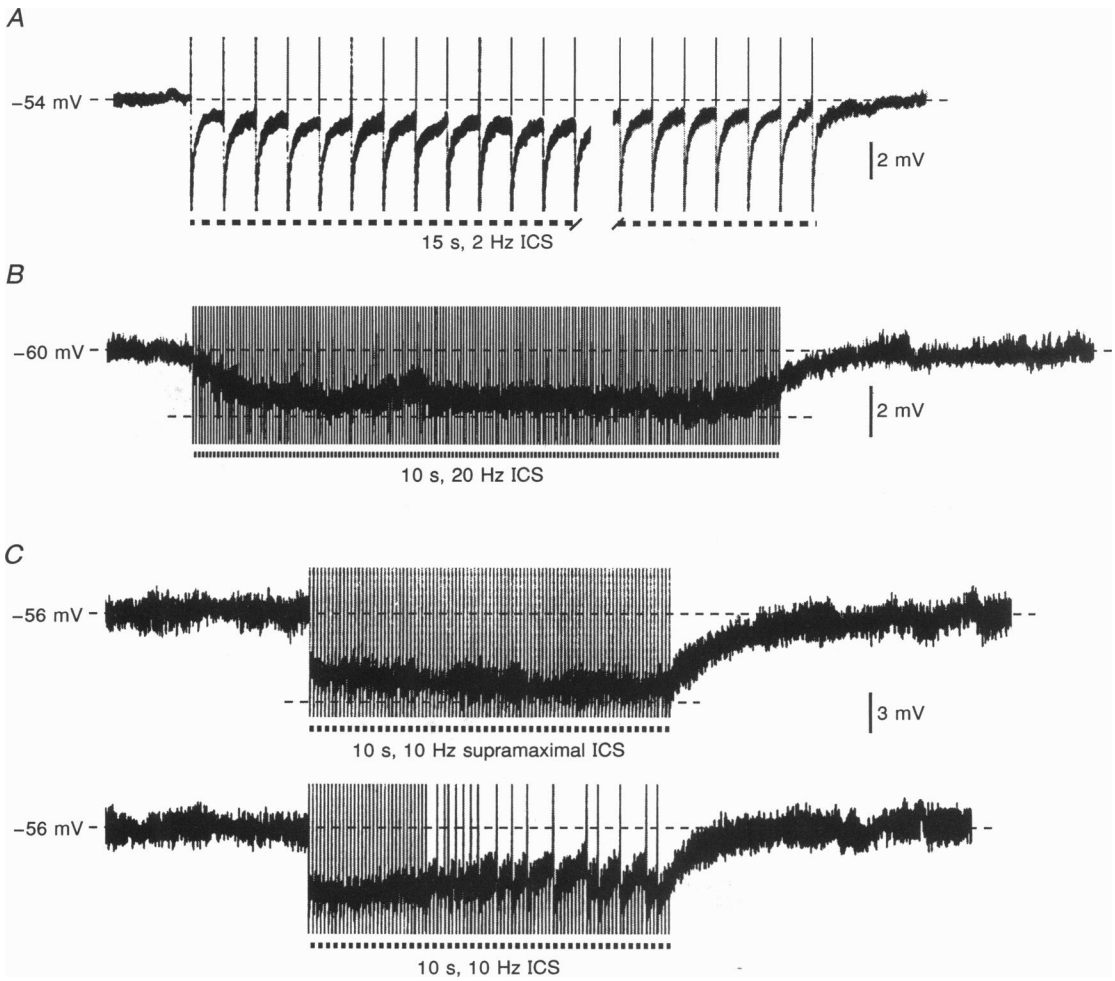

Figure 2. Hyperpolarizing shift evoked by repetitive intracellular stimulus pulses

Hyperpolarizing shift evoked by suprathreshold intracellular stimulation (ICS; dashed lines, spike amplitude clipped) delivered at 2 Hz (*A*) and 20 Hz (*B*). *C*, in this cell, stimulation pulses were either well suprathreshold (upper trace) or just-suprathreshold (lower trace). Spike failure in the latter case led to a relaxation of the hyperpolarizing shift (upward drift of the membrane potential).

Table 2. Peak amplitude and duration of the hyperpolarizing shift evoked by a 10 s train of suprathreshold intracellular stimulus pulses delivered at 10 or 20 Hz

Neuron type	Number of cells	Stimulation frequency (Hz)	Peak amplitude (mV)	Recovery time (s)
$A_0 + A_{inf}$	18*	10	2·1 ± 1·6	2·7 ± 2·4
			$P < 0·001$	$P < 0·005$
$A_0 + A_{inf}$	Same 18	20	3·7 ± 2·6	6·7 ± 5·7
A_0	12†	20	2·2 ± 1·7	3·7 ± 2·5
			$P < 0·005$	$P < 0·05$
A_{inf}	7	20	5·9 ± 2·1	13·6 ± 10·9

Values are means ± S.D. * Eleven A_0 neurons, seven A_{inf} neurons. † Six of these cells had prolonged AHP to single pulses. For these, peak amplitude was 2·8 ± 1·7 mV, recovery time was 3·3 ± 2·6 s. *P* values are based on two-tailed Mann–Whitney *U* tests.

After-effects of conditioning tetani (DRG cross-excitation)

The presence of a hyperpolarizing shift triggered by spiking does not rule out the possibility of a direct contribution to after-suppression by the process (e.g. neurotransmitter) responsible for the excitation in the first place. In lieu of testing this for all possible excitatory stimuli, we focused on the after-suppression that follows excitation due to activity of neighbouring neurons that share a single DRG. This phenomenon is particularly salient as all natural stimuli excite more than one neuron in a given DRG, and hence mutual interactions among neighbouring neurons are a part of normal sensory signalling.

In nearly all of the neurons tested (90 of 95; 95%; 51 of 54 A_0, 39 of 41 A_{inf}) conditioning stimulation of the axons of

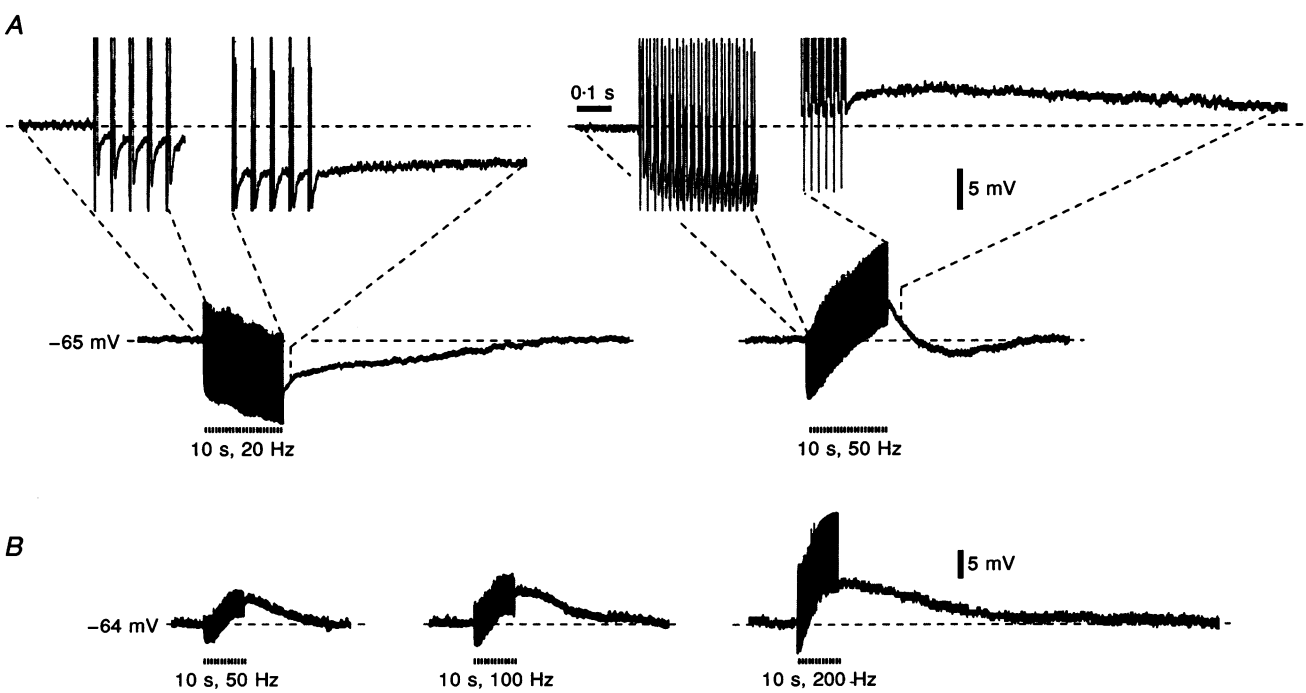

Figure 3. Prolonged spike-evoked hyperpolarizing and depolarizing shifts

A, stimulated at 20 Hz this cell showed a prolonged hyperpolarizing shift. Stimulated at 50 Hz there was initial hyperpolarization, which then developed into a depolarizing shift. The insets show the first few and last few stimuli in the tetanus. *B*, this cell showed a very brief hyperpolarizing shift followed by a more prolonged depolarizing shift. The amplitude of the depolarizing shift increased with increasing stimulation frequency. All spikes are clipped.

neighbouring afferents evoked transient depolarization (Fig. 5*B*). Peak depolarization amplitude ranged from 0·5 to 25 mV (mean, 3·2 ± 2·7 mV). We call this 'DRG cross-depolarization' (Utzschneider, Kocsis & Devor, 1992). *In vivo* (Wall & Devor, 1990), and under appropriate conditions *in vitro* (Amir & Devor, 1995), activity in neighbouring neurons evokes or accelerates spiking in the cell under study ('cross-excitation'). DRG cross-depolarization, and consequent cross-excitation, are due to chemical mediators released within the DRG (Amir & Devor, 1996). Here we ask whether cross-depolarization is followed by after-suppression in the absence of spiking.

Whenever neurons showed cross-depolarization without spiking, membrane potential returned directly to baseline after the end of the conditioning tetanus, with no overshoot in the hyperpolarizing direction (Fig. 5*B*, see also Utzschneider *et al.* 1992). Conditioning was associated with a net increase in R_{in} (43 of 49 cells tested; 26 of 29 A_0, 17 of 20 A_{inf}; Amir & Devor, 1996). This is best illustrated in experiments in which the cross-depolarization was minimal, or was balanced out using intracellular current injection. R_{in}, too, returned monotonically to baseline at the end of the conditioning train (Fig. 5*C*). There was never an overshoot phase of decreased R_{in} following the tetanus.

Finally, during conditioning there was a significant increase in firing probability ('cross-excitation') in 41 of 57 cells tested (29 of 40 A_0, 12 of 17 A_{inf}; Amir & Devor, 1996). However, in no case did firing probability fall below baseline in the aftermath of conditioning (Fig. 5*D*). Thus, cross-depolarization is not followed by hyperpolarization, altered R_{in}, or decreased excitability, three parameters that might have been expected to accompany after-suppression. We infer that after-suppression is not a direct effect of the process responsible for cell-to-cell coupling within DRGs, but rather is related to the accelerated spike discharge evoked by conditioning tetani.

Intermittence (bursting) generated by the hyperpolarizing shift

Stimulus pulse-evoked firing

When the intracellular stimulation pulses used were initially just-suprathreshold, they often became subthreshold during the course of the hyperpolarizing shift. The result was spike failure and termination of the shift. Membrane potential then returned towards baseline and spiking resumed. This refreshed the hyperpolarizing shift. The net result was cycling between spiking and spike failure, i.e. bursting (Fig. 6). This continued for the duration of the tetanus.

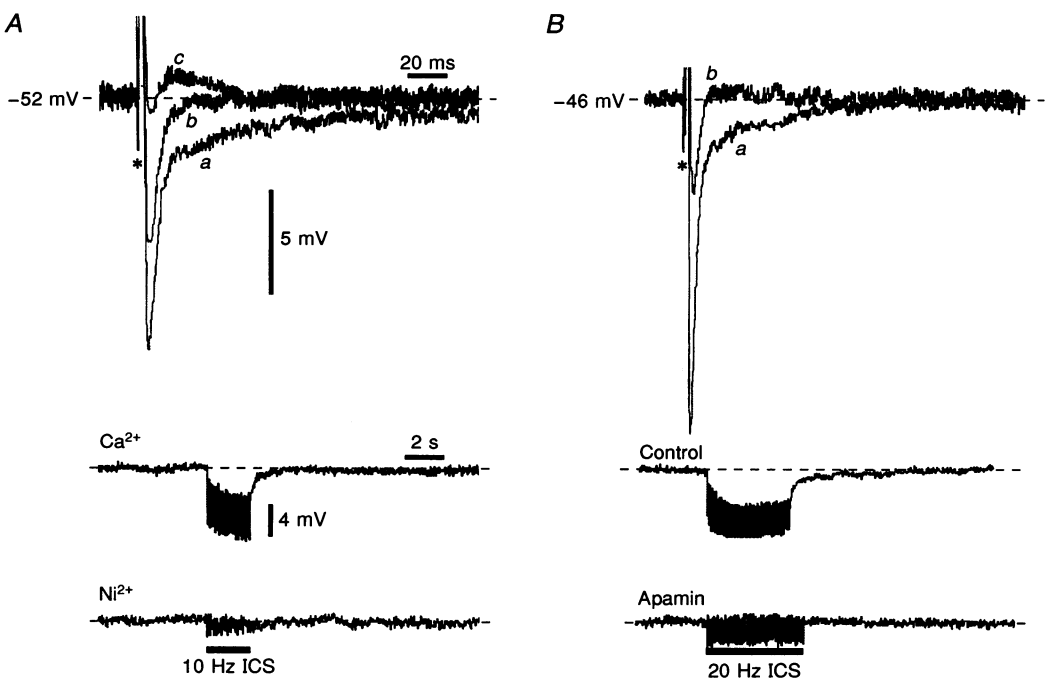

Figure 4. AHP and the spike-evoked hyperpolarizing shift are attenuated by blockers of g_{Ca} and $g_{K(Ca)}$

Spikes were evoked by single stimulus pulses to the nerve (*). Replacing Ca^{2+} ions with Ni^{2+} (*A*), or adding the $g_{K(Ca)}$ blocker apamin (5 nM; *B*) strongly attenuated both the brief and the prolonged phases of the AHP (traces *a* are baseline; in *A*, trace *b* is after 5 min and trace *c* is after 8 min; in *B*, trace *b* is after 10 min). A depolarizing after-potential was revealed in the cell in trace *A c*. Lower panels show that the spike-evoked hyperpolarizing shift was eliminated following application of blockers (*A*, after 8 min; *B*, after 10 min). Spikes are truncated (upper panels) or filtered out (lower panels). Both cells are A_{inf} neurons.

Although spike-evoked hyperpolarization shifted the cell away from threshold, this was not necessarily the sole basis for the suppression in firing probability. In about one-third of the cells spike failure began well after the hyperpolarization had reached a plateau, and sometimes even after it had begun to fall back from its peak (Fig. 2*C* bottom, and Fig. 6). In one cell, spike failure occurred without a noticeable hyperpolarization. The latency until spike failure appeared to vary more with the number of stimulus pulses delivered than with the exact value of the membrane potential (Fig. 6*A* *vs.* *B*). Finally, in some cells suppression was seen in the presence of apamin or Ca^{2+} channel blockers after the hyperpolarizing shift had been eliminated. Luscher *et al.* (1994) noted that spiking in DRG cells may activate a membrane conductance(s) not reflected in additional potential change. Such a conductance is expected to shunt the current of test pulses and hence reduce firing probability.

Spontaneous firing

On occasion we encountered cells with spontaneous activity. So far, all have been A_0 neurons. Firing was typically in an

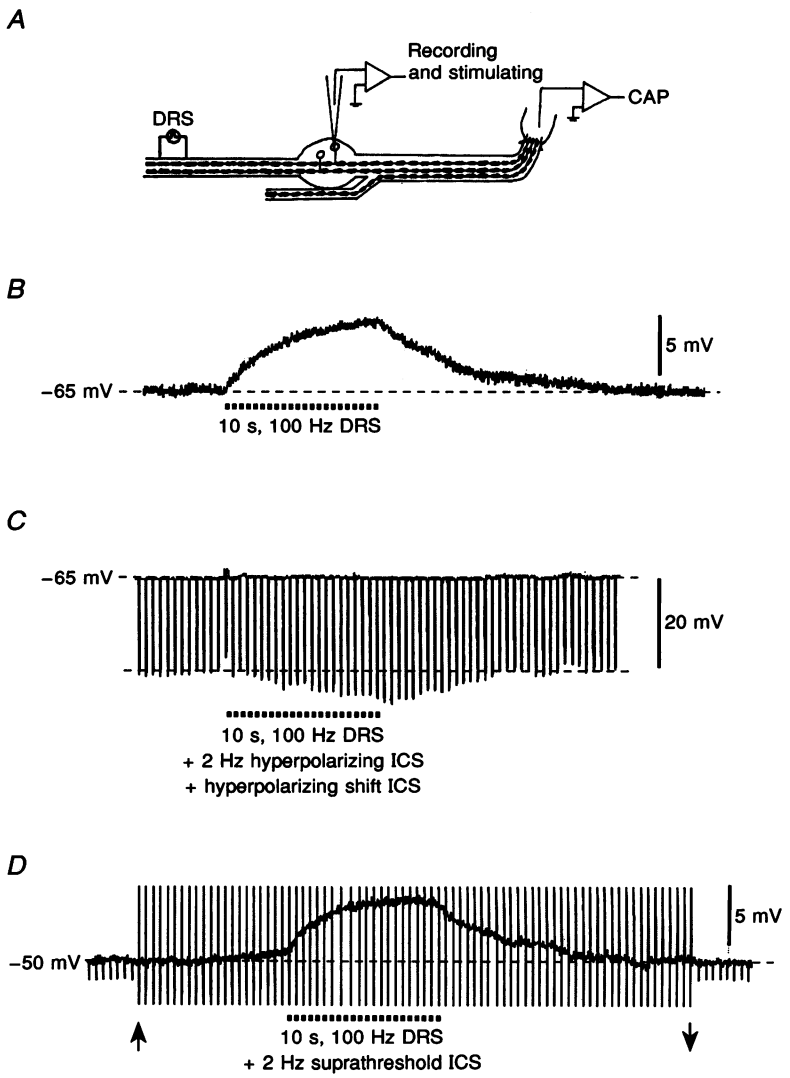

Figure 5. Cross-excitation

A, recording set-up with DR stimulation (DRS), suction electrode for monitoring the evoked compound action potential (CAP), and intracellular microelectrode for recording and stimulating DRG neurons. *B*, conditioning stimulation at DR (horizontal dashed line, subthreshold for the axon of the impaled neuron) evoked cross-depolarization followed by return to baseline, with no after-hyperpolarization. *C*, hyperpolarizing test pulses delivered intracellularly (ICS) were used to monitor R_{in} during conditioning. Cross-depolarization was balanced out by injecting hyperpolarizing current intracellularly. Conditioning caused an increase in R_{in} (same cell as in *B*). *D*, between the arrows stimulus pulses just-suprathreshold for evoking spikes were delivered intracellularly (spike amplitude clipped). Conditioning evoked cross-depolarization, but there was no subsequent decrease in firing probability.

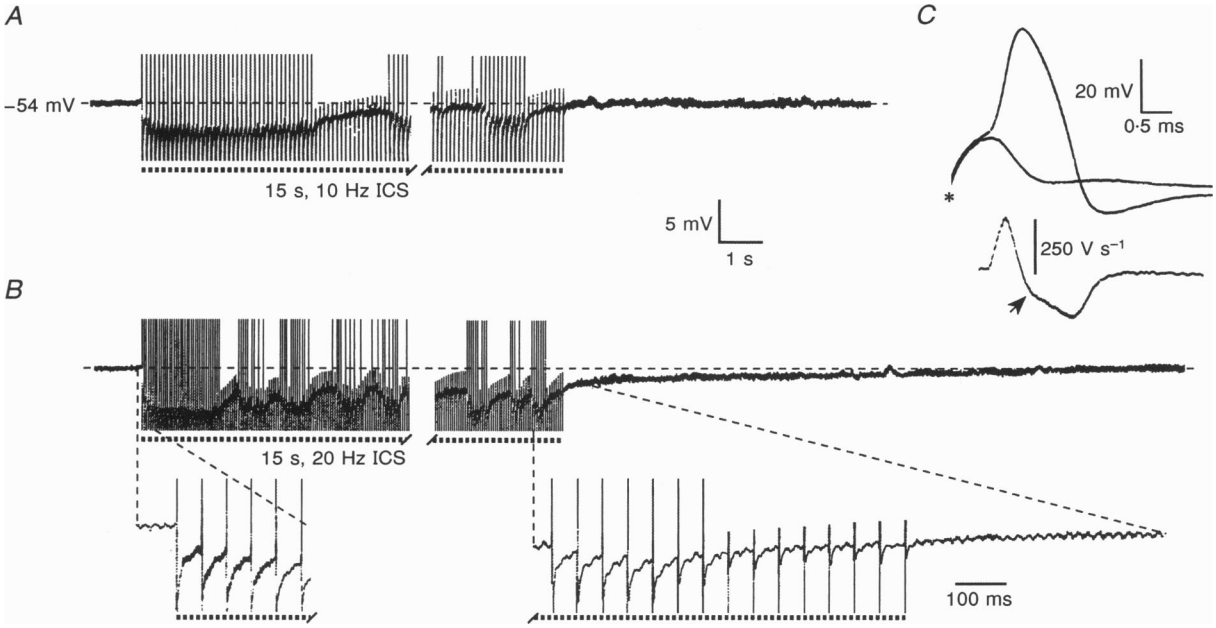

Figure 6. Effect of stimulation frequency on spike burst pattern

Identical just-suprathreshold intracellular stimulus (ICS) trains were delivered at 10 Hz in *A* and 20 Hz in *B*. The rate of development of the hyperpolarizing shift, its steady-state amplitude, the time to first spike failure, and the frequency of bursting all varied with stimulus frequency. *C* shows the waveform of the soma spike (just-subthreshold and just-suprathreshold) including a differentiated voltage record illustrating the inflection on the falling limb of the spike (arrow).

'on–off' pattern resembling that previously reported in *in vivo* preparations (Fig. 7; Wall & Devor, 1983), but with shorter interspike intervals during on-periods (5–15 ms compared with 20–100 ms). Spike bursts appeared to arise from spontaneous subthreshold membrane oscillations (Amir & Devor, 1995). These gradually increased in amplitude until, when they reached 3–6 mV, spiking began. The spiking occasioned a membrane potential shift in the hyperpolarizing direction, accompanied by an increase in interspike intervals and a decrease in spike amplitude (Fig. 7). After 70–700 ms, firing suddenly ceased. Membrane potential at this point was hyperpolarized by 1·0–3·0 mV compared with its value just before the burst began, and membrane oscillations were small. The interval between bursts ranged from 0·1 to 4·0 s. During this silent period subthreshold membrane potential oscillations gradually increased in

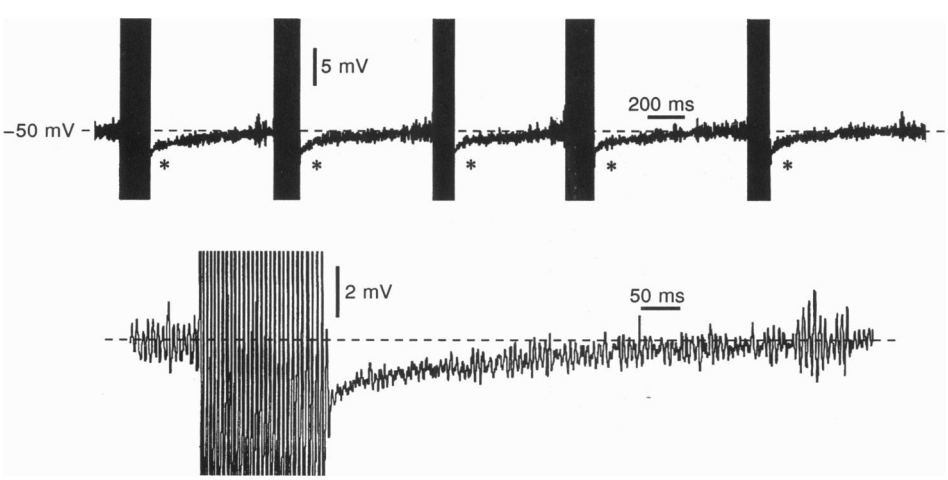

Figure 7. After-hyperpolarizing shifts induce on–off firing

After-hyperpolarizing shifts (*) induced on–off firing in this spontaneously active A_0 neuron. The first burst is shown in the lower trace on a more sensitive scale. Note voltage oscillations in membrane potential.

amplitude once again until spiking resumed, completing the burst cycle (Fig. 7).

Afferent nerve activity and dynamic control of neuron membrane potential

In the normal functioning of primary afferent neurons, impulses originate at the peripheral receptor ending and propagate past the DRG, usually invading the cell soma. This is expected to engage two opposing processes in the DRG neuron: cross-depolarization and the spike-evoked hyperpolarizing shift. To determine which is dominant, stimulus trains were delivered to the sciatic nerve or the DR. Nerve stimulation subthreshold for the axon of the impaled neuron only evoked cross-depolarization (Figs 5*B* and 8*A*, upper trace). Using supramaximal pulses, which stimulate the axon of the impaled neuron as well as most of its neighbours, the net outcome was almost always hyperpolarization (13 of 14 neurons tested; Fig. 8*A*, lower trace).

There is a dynamic interplay between the two processes. For example, in the experiment illustrated in Fig. 8*B*, cross-depolarization was replaced by hyperpolarization when the conditioning stimulus current was briefly increased so as to recruit the axon of the impaled cell. Subsequent return toward cross-depolarization was momentarily interrupted when the impaled neuron fired a few spikes, resulting in dynamic fluctuations in the membrane potential of the cell. The membrane potential of the neuron reflects an on-going balance between its own activity and that of its neighbours.

A different perspective on the the dynamic interplay of cross-depolarization and spike-evoked suppression is shown in Fig. 9. Weak nerve stimulation appeared to activate exclusively the axon of the impaled unit (Fig. 9*B* and *C*), and repetitive stimulation at this intensity evoked a hyperpolarizing shift identical to that evoked by intracellular tetanic stimulation (Fig. 9*E*, upper two traces). However, when the intensity of the nerve stimulation was increased to recruit neighbouring axons (Fig. 9*D*), the hyperpolarizing shift was attenuated (Fig. 9*E*, lower trace).

DISCUSSION

We have shown that repetitive firing of DRG A-neurons triggers a prolonged hyperpolarizing shift. The hyperpolarizing shift is capable of suppressing accelerated firing triggered by any of a range of different excitatory processes (see Introduction). On the other hand, the process responsible

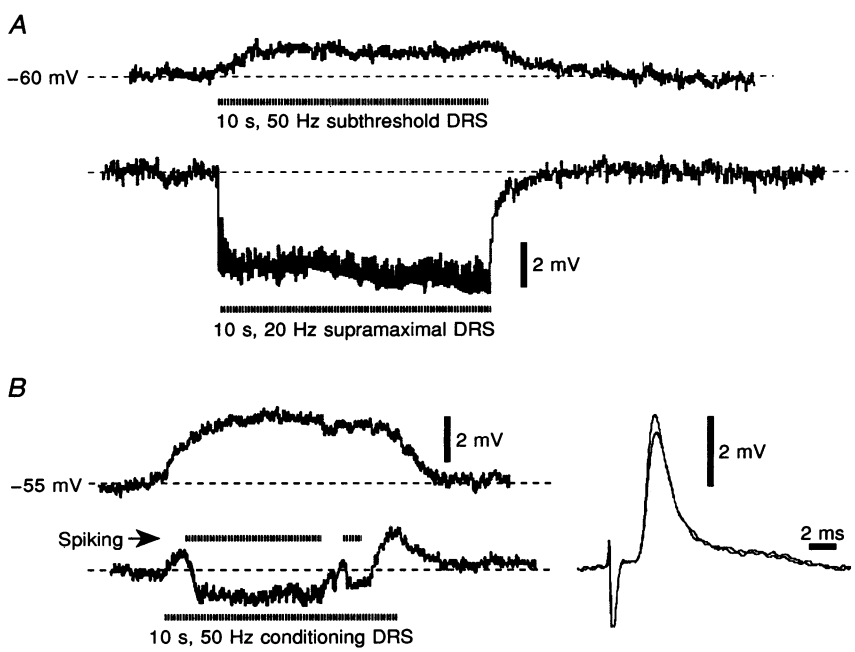

Figure 8. The spike-evoked hyperpolarizing shift overcomes cross-depolarization

A, a conditioning train delivered to the DR at an intensity just-subthreshold for the axon of the impaled cell, but suprathreshold for many neighbours, evoked cross-depolarization (upper trace). When stimulus intensity was increased to recruit the impaled cell's axon, spiking (not visible in the record) evoked a hyperpolarizing shift. *B*, as in *A*, subthreshold DR stimulation evoked cross-depolarization (left, top). Stimulation intensity was then variably brought to threshold so as to initiate spiking of the impaled neuron. During periods of spiking, membrane potential shifted in the hyperpolarizing direction (left, bottom). Traces on the right, which show the CAP evoked using currents just-sub- and just-suprathreshold for the axon of the impaled neuron, indicate the small number of additional axons recruited in the process. In *A* and *B* soma spikes were removed from the traces in order to permit better visualization of the underlying membrane potential change.

for excitation could, itself, produce delayed suppression. One example, DRG cross-excitation, was examined as a test case. Conditioning tetani delivered to afferent neurons that share a DRG with the impaled neuron induced excitatory cross-depolarization. However, in the absence of neuronal spiking, the coupling process in itself did not evoke after-hyperpolarization, or a post-tetanic change in R_{in} or firing probability. We conclude that it is not directly responsible for after-suppression. Rather, in the event of cross-excitation with cell spiking, after-suppression is an intrinsic process associated with elevated firing rate. Since spike-evoked after-suppression is likely to be engaged no matter what the initial cause of the accelerated firing, we infer that depressed firing rate in the wake of excitatory stimulation in general is also due, at least in part, to the spike-evoked suppression mechanism.

AHP and the spike-evoked hyperpolarizing shift

Nearly all neurons tested showed an AHP following single soma spikes, and in over one-third the AHP was prolonged. Both brief and prolonged AHPs are well known in DRG neurons of rats and other vertebrate species (Gallego, 1983; Harper & Lawson, 1985; Leonard & Wickelgren, 1985; Fulton, 1987; Villiere & McLachlan, 1996). When stimulated

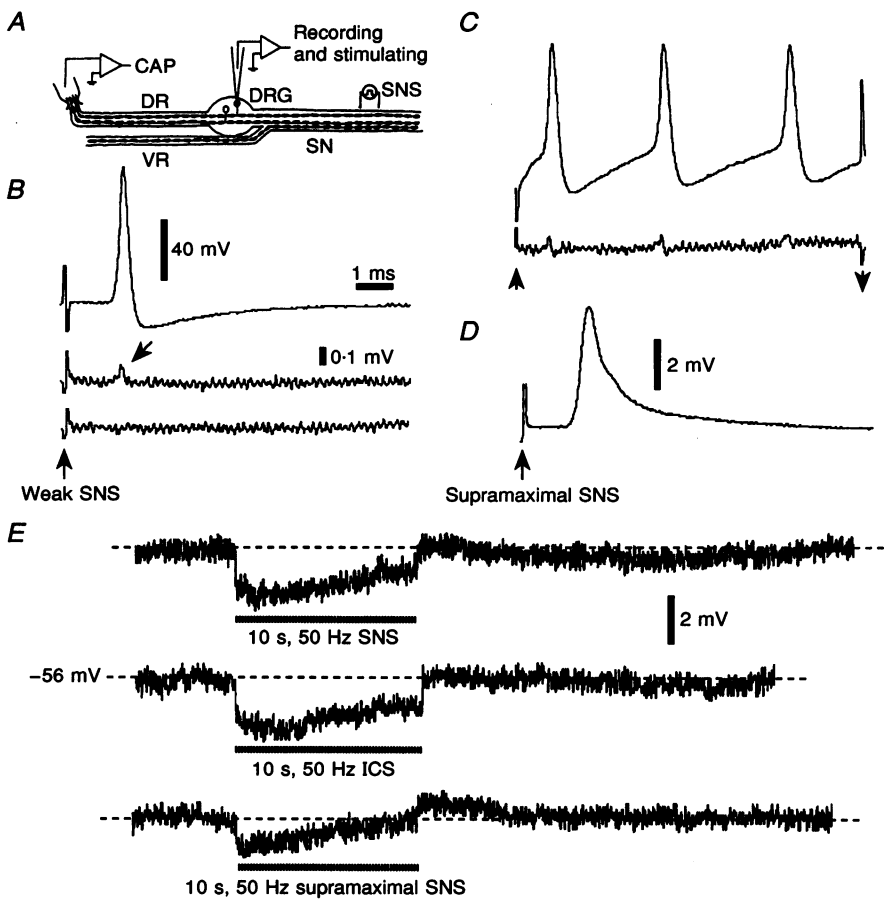

Figure 9. Superimposition of cross-depolarization onto spike-evoked hyperpolarizing shift

A, the experimental protocol (see Methods): CAP, compound action potential; SN, sciatic nerve; SNS, sciatic nerve stimulation; VR, ventral root. Distances: SNS to Recording and stimulating micropipette, 24 mm; Recording and stimulating micropipette to CAP, 5 mm. *B*, weak nerve stimulation (Weak SNS) activated the impaled neuron, and few if any others. The upper trace shows the intracellular spike using just-suprathreshold nerve stimulation. The lower two traces show the simultaneously recorded all-or-none response (oblique arrow) on the DR suction electrode (CAP) using just-suprathreshold and just-subthreshold stimulation current. *C*, corresponding signals were recorded intracellularly and from the DR during repetitive firing of the cell evoked by a step depolarizing pulse applied intracellularly (between arrows). *D* shows the DR CAP signal evoked by supramaximal nerve stimulation (Supramaximal SNS), which is far larger than that evoked by stimulating the impaled neuron alone. *E*, repetitive, just-suprathreshold nerve stimulation (SNS, top trace), sufficient only to drive the impaled neuron, evoked a hyperpolarizing shift similar in amplitude to that evoked by intracellular stimulation (ICS, middle trace). When nerve stimulation intensity was increased to supramaximal (bottom trace), the hyperpolarization was attenuated due to the addition of cross-depolarization. Spikes were removed from the traces in *E*.

repetitively ($\geqslant 5$ Hz), nearly all neurons tested showed a hyperpolarizing shift. In the cells with a prolonged AHP this is most easily explained as temporal summation of AHPs. However, the shift often occurred even when the AHP appeared to be considerably shorter than the interval between stimulus pulses. This suggests that temporal summation of AHPs may not be the only mechanism involved.

Detailed analysis by others has shown that the prolonged AHP in vertebrate DRG neurons is due to $g_{K(Ca)}$ activated by Ca^{2+} entry during spike activity (e.g. Gorke & Pierau, 1980; Gallego, 1983; Leonard & Wickelgren, 1985). Our results are consistent with this mechanism. The inflection on the falling phase of A_{inf} spikes reflects a voltage-sensitive Ca^{2+} current (e.g. Gorke & Pierau, 1980; Gallego, 1983; Leonard & Wickelgren, 1985) and spiking increases intracellular Ca^{2+} concentration (e.g. Luscher *et al.* 1994). Correspondingly, we found that DRG cells with an inflection (A_{inf} cells) had a more pronounced post-spike AHP than cells without an inflection (A_0 cells). They also had a more prominent tetanus-triggered hyperpolarizing shift. The g_{Ca} blockers Co^{2+} and Ni^{2+}, and the selective $g_{K(Ca)}$ blocker apamin, reduced or eliminated not only the AHP, but also the hyperpolarizing shift. We infer that the hyperpolarizing shift primarily reflects Ca^{2+} accumulation and persistent activation of $g_{K(Ca)}$. However, we cannot rule out a minor contribution by other mechanisms, e.g. Na^+ pumping or a Na^+-dependent K^+ current (Rang & Ritchie, 1968; Schwindt, Spain & Crill, 1989; Gordon, Kocsis & Waxman, 1990; Hainmann, Bernheim, Bertrand & Bader, 1990), especially in those cells where Co^{2+}, Ni^{2+}, or apamin did not block the hyperpolarizing shift completely.

Surprisingly, we found no difference in spike duration between A_0 neurons that had a prolonged AHP and ones that did not ($P > 0{\cdot}2$). Moreover, most A_0 neurons showed at least a small hyperpolarizing shift even though they did not have a detectable inflection. Ni^{2+} abolished the hyperpolarizing shift in at least one A_0 neuron that did not have a prolonged AHP. In another A_0 neuron that did have a prolonged AHP, apamin blocked the AHP and diminished the hyperpolarizing shift. These findings suggest that A_0 neurons have a Ca^{2+} component to their action potential despite the lack on an inflection. Consistent with this possibility, spike amplitude was reduced by Ni^{2+} in the two A_0 neurons tested (see also Villiere & McLachlan, 1996).

Spike-evoked suppression and the patterning of spontaneous ectopic discharge in primary afferent neurons

Threshold suppression triggered by spiking can account for several of the peculiarities of spontaneous ectopic discharge in DRGs. Moreover, since similar membrane conductances are likely to be present in other parts of the neuron, the same arguments are likely to hold for ectopic spike patterning at nerve injury sites, such as nerve-end neuromas and in-continuity chronic nerve constriction sites (Devor, 1994; Tal & Eliav, 1996). The most common pattern for spontaneous ectopic discharge in injured afferent neurons is tonic rhythmic firing. In light of the present results, spontaneous firing frequency must reflect an equilibrium between the excitatory processes responsible for the ectopic electrogenesis (Devor *et al.* 1994), and the spike-evoked suppression that results from it.

If spike discharge is at equilibrium near the unit's threshold for rhythmic firing (Matzner & Devor, 1992), any perturbation that either accelerates or suppresses the firing can initiate bursting. Indeed, bursting (on–off firing) is the second most commonly observed pattern of spontaneous ectopic firing *in vivo*. Consistent with this hypothesis for the origin of bursting *in vivo*, we showed that the spike-evoked suppression mechanism can transiently terminate spontaneous activity in DRG neurons *in vitro*, setting them into an on–off, bursty firing pattern (Figs 6 and 7). Finally, as already noted, spike-evoked suppression can account for the transient quenching which frequently follows mechanical, ischaemia and drug-induced DRG excitation *in vivo* (see references in the Introduction).

Functional implications of cross-excitation and spike-evoked suppression

Normal sensation

Only a low level of on-going spike activity originates in the DRG of nerve-intact animals (Wall & Devor, 1983; Burchiel, 1984*a*; Study & Kral, 1996). This background activity is presumed to be of little functional consequence, although it might contribute to a liminal sense of body image in the intact individual, and to the sensation of a 'normal' phantom limb when nerves are blocked with local anaesthetics (Melzack & Bromage, 1973; Devor, 1996).

More significantly, our data suggest that the membrane potential of most primary afferent neurons is dynamically modulated by afferent activity arising in the periphery, not only in the cell's own RF, but also in that of neighbours (Figs 8 and 9). Consider a probe gently stroked across the skin. For any given neuron in the DRG, as the probe approaches the neuron's RF, spikes generated in neighbouring cutaneous afferents invade the ganglion as they propagate centrally towards the CNS. This induces cross-depolarization. As soon as the probe enters the RF of the neuron in question it begins to fire, shifting the net influence from depolarization to spike-evoked hyperpolarization. Finally, as the probe leaves the RF, cross-depolarization takes over once again.

It is likely that different afferent types engage, and are engaged by, cross-depolarization and spike-evoked hyperpolarization with different potency. Likewise, the dynamic interplay of these two opponent processes will be affected by stimulus texture and velocity, and the efficiency of soma spike invasion. In short, the membrane potential of each DRG neuron, at each moment in time, reflects a complex integral of the stimulus configuration imposed on its RF, and

those of its neighbours. It remains to be determined whether subthreshold membrane potential modulation associated with afferent input from the periphery has any practical consequences for sensation, in the absence of ectopic spike generation in the DRG, for example, by affecting cell metabolism or gene expression.

Pathophysiology

If the DRG were pathologically hyperexcitable, as a result of nerve injury or disease, for example (Wall & Devor, 1983; Burchiel, 1984*a*, *b*; Kajander *et al.* 1992; Study & Kral, 1996), cross-excitation could add to the spontaneous ectopic barrage originating there, and also amplify normal afferent input. Indeed, under appropriate conditions, coupling among DRG neurons could enter a positive feedback mode. That is, a nucleus of activity, perhaps initiated in the skin, might kindle spiking in neighbouring neurons, which would cross-excite additional neighbours, ultimately igniting most or all of the ganglion in an explosive 'chain reaction'. Rappaport & Devor (1994) proposed that this process underlies touch-triggered paroxysmal pain attacks in trigeminal and other neuralgias. Consistent with this hypothesis, trigeminal lightning attacks are typically followed by a brief 'refractory period' during which the trigger mechanism is blocked (Kugelberg & Lindblom, 1959). The spike-evoked suppression process described here is ideally suited to account for this refractoriness.

Amir, R. & Devor, M. (1995). Membrane oscillations trigger spontaneous activity and cross-excitation in sensory neurons in the rat. *Israel Journal of Medical Sciences* **31**, 727.

Amir, R. & Devor, M. (1996). Chemically-mediated cross-excitation in rat dorsal root ganglia. *Journal of Neuroscience* **16**, 4733–4741.

Burchiel, K. J. (1984*a*). Spontaneous impulse generation in normal and denervated dorsal root ganglia: sensitivity to alpha-adrenergic stimulation and hypoxia. *Experimental Neurology* **85**, 257–272.

Burchiel, K. J. (1984*b*). Effects of electrical and mechanical stimulation on two foci of spontaneous activity which develop in primary afferent neurons after peripheral axotomy. *Pain* **18**, 249–265.

Devor, M. (1994). The pathophysiology of damaged peripheral nerves. In *Textbook of Pain*, 3rd edn, chap. 4, ed. Wall, P. D. & Melzack, R., pp. 79–100. Churchill–Livingston, London.

Devor, M. (1996). Phantom pain as an expression of referred and neuropathic pain. In *Phantom Pain*, chap. 2, ed. Sherman, R. A., Devor, M., Casey Jones, D. E., Katz, J. & Marbach, J. J., pp. 33–57. Plenum Press, New York.

Devor, M., Janig, W. & Michaelis, M. (1994). Modulation of activity in dorsal root ganglion neurons by sympathetic activation in nerve-injured rats. *Journal of Neurophysiology* **71**, 38–47.

Devor, M. & Wall, P. D. (1990). Cross-excitation among dorsal root ganglion neurons in nerve injured and intact rats. *Journal of Neurophysiology* **64**, 1733–1746.

Fowler, J. C., Greene, R. & Weinreich, D. (1985). Two calcium-sensitive spike after-hyperpolarizations in visceral sensory neurones of the rabbit. *Journal of Physiology* **365**, 59–75.

Fulton, B. P. (1987). Postnatal changes in conduction velocity and soma action potential parameters of rat dorsal root ganglion neurones. *Neuroscience Letters* **73**, 125–130.

Gallego, R. (1983). The ionic basis of action potentials in petrosal ganglion cells of the cat. *Journal of Physiology* **342**, 591–602.

Gordon, T. R., Kocsis, J. & Waxman, S. G. (1990). Electrogenic pump (Na^+/K^+-ATPase) activity in rat optic nerve. *Neuroscience* **37**, 829–837.

Gorke, K. & Pierau, F. K. (1980). Spike potentials and membrane properties of dorsal root ganglion cells in pigeons. *Pflügers Archiv* **386**, 21–28.

Hainmann, C., Bernheim, L., Bertrand, D. & Bader, C. R. (1990). Potassium current activated by intracellular sodium in quail trigeminal ganglion neurons. *Journal of General Physiology* **95**, 961–979.

Harper, A. A. & Lawson, S. N. (1985). Electrical properties of rat dorsal root ganglion neurones with different peripheral nerve conduction velocities. *Journal of Physiology* **359**, 47–63.

Howe, J. F., Loeser, J. D. & Calvin, W. H. (1977). Mechanosensitivity of dorsal root ganglia and chronically injured axons: a physiological basis for the radicular pain of nerve root compression. *Pain* **3**, 25–41.

Kajander, K. C., Wakisaka, S. & Bennett, G. J. (1992). Spontaneous discharge originates in the dorsal root ganglion at the onset of a painful peripheral neuropathy in the rat. *Neuroscience Letters* **138**, 225–228.

Koerber, H. R. & Mendell, L. M. (1992). Functional heterogeneity of dorsal root ganglion cells. In *Sensory Neurons*, ed. Scott, S. A., pp. 77–96. Oxford University Press, New York.

Kugelberg, E. & Lindblom, U. (1959). The mechanism of the pain in trigeminal neuralgia. *Journal of Neurology, Neurosurgery and Psychiatry* **22**, 36–43.

Leonard, J. P. & Wickelgren, W. O. (1985). Calcium spike and calcium dependent potassium conductance in mechanosensory neurons of the lamprey. *Journal of Neurophysiology* **53**, 171–182.

Luscher, C., Streit, J., Lipp, P. & Luscher, H. R. (1994). Action potential propagation through embryonic dorsal root ganglion cells in culture. II. Decrease of conduction reliability during repetitive stimulation. *Journal of Neurophysiology* **72**, 634–643.

Lutzky, L., Aizer, F. & Mor, N. (1984). The 'Sabra' rat: definition of a laboratory animal. *Israel Journal of Medical Sciences* **20**, 603–612.

Matzner, O. & Devor, M. (1992). Na^+ conductance and the threshold for repetitive neuronal firing. *Brain Research* **597**, 92–98.

Mayer, M. L. (1985). A calcium-activated chloride current generates the after-depolarization of rat sensory neurones in culture. *Journal of Physiology* **364**, 217–239.

Melzack, R. & Bromage, P. R. (1973). Experimental phantom limbs. *Experimental Neurology* **39**, 261–269.

Rang, H. P. & Ritchie, J. M. (1968). On the electrogenic sodium pump in mammalian non-myelinated nerve fibres and its activation by various external cations. *Journal of Physiology* **196**, 183–221.

Rappaport, Z. H. & Devor, M. (1994). Trigeminal neuralgia: the role of self sustaining discharge in the trigeminal ganglion. *Pain* **56**, 127–138.

Schwindt, P. C., Spain, W. J. & Crill, W. E. (1989). Long-lasting reduction of excitability by a sodium-dependent potassium current in cat neocortical neurons. *Journal of Neurophysiology* **61**, 233–244.

Sheen, K. & Chung, J. M. (1993). Signs of neuropathic pain depend on signals from injured fibers in a rat model. *Brain Research* **610**, 62–68.

SHINDER, V. & DEVOR, M. (1994). Structural basis of neuron-to-neuron cross-excitation in dorsal root ganglia. *Journal of Neurocytology* **23**, 515–531.

STUDY, R. & KRAL, M. G. (1996). Spontaneous action potential activity in isolated dorsal root ganglion neurons from rats with a painful neuropathy. *Pain* **65**, 235–242.

TAL, M. & ELIAV, E. (1996). Abnormal discharge originates at the site of nerve injury in experimental constriction neuropathy (CCI) in the rat. *Pain* **64**, 511–518.

UTZSCHNEIDER, D., KOCSIS, J. & DEVOR, M. (1992). Mutual excitation among dorsal root ganglion neurons in the rat. *Neuroscience Letters* **146**, 53–56.

VILLIERE, V. & MCLACHLAN, E. M. (1996). Electrophysiological properties of neurons in intact rat dorsal root ganglia classified by conduction velocity and action potential duration. *Journal of Neurophysiology* **76**, 1924–1941.

WALL, P. D. & DEVOR, M. (1983). Sensory afferent impulses originate from dorsal root ganglia as well as from the periphery in normal and nerve injured rats. *Pain* **17**, 321–339.

XIE, Y., ZHANG, J., PETERSEN, M. & LA MOTTE, R. H. (1995). Functional changes in dorsal root ganglion cells after chronic nerve constriction in the rat. *Journal of Neurophysiology* **73**, 1811–1820.

YOON, Y. W., NA, H. S. & CHUNG, J. M. (1996). Contributions of injured and intact afferents to neuropathic pain in an experimental rat model. *Pain* **64**, 27–36.

Acknowledgements

We thank J. Kocsis, P. D. Wall and Y. Yarom for useful comments on the manuscript. This work was supported by grants from the German–Israeli Foundation for Research and Development, the United States–Israel Binational Science Foundation, and the Israel Ministry of Science and Arts.

Author's email address

M. Devor: marshlu@vms.huji.ac.il

Received 29 November 1996; accepted 19 February 1997.